JOURNAL OF MATERIALS SCIENCE 30 (1995) 4043–4048

R-curve behaviour of sintered silicon nitride

Y. W. KIM*, M. MITOMO
National Institute for Research in Inorganic Materials, Ibaraki 305, Japan

N. HIROSAKI
Materials Research Laboratory, Nissan Research Centre, Nissan Motor Company Ltd, Yokosuka 237, Japan

R-curves for two *in situ* reinforced silicon nitrides A and B of different microstructures were determined by three different characterization methods. The saturated crack growth resistance was found to be 5.2, 7.2 and 9.2 MPa $m^{1/2}$ for silicon nitride A and 5.8, 8.0 and 10.0 MPa $m^{1/2}$ for silicon nitride B, respectively, by indentation, indentation–crack growth, and indentation–strength methods. The rising behaviour of *R*-curves was also found to depend on the characterization method. These results indicate that care should be taken in interpreting and utilizing *R*-curves evaluated from different characterization methods and an *R*-curve characterization method with appropriate qualifiers is needed for rising *R*-curve materials.

1. Introduction

Sintered silicon nitride containing rod-like grains has a high fracture toughness because of a bridging [1] or a crack-deflection [2] toughening mechanism. The *in situ* reinforced silicon nitride ceramics are fabricated from β-Si_3N_4 starting powder [3–6] as well as Si_3N_4 powder with a high α content [7–9]. The *in situ* reinforced silicon nitride ceramics exhibit increasing resistance to fracture with crack extension [10–12]. This behaviour is frequently referred to as "*R*-curve" behaviour and they are referred to as *R*-curve materials. *R*-curve behaviour arises because additional energy is required in addition to that needed at the crack tip to propagate the crack. The additional energy is required to overcome, perhaps, the restraining forces of ligaments in the wake of the crack. A tortuous crack path such as crack bridging [1] and crack deflection [2] possibly constitutes a systematic increase of the fracture resistance. Many other ceramics, including zirconia [13], alumina [14], and silicon carbide whisker-reinforced alumina [15], also exhibit *R*-curve behaviour.

It has been shown that the shape of the *R*-curve dictates the strength variability and damage tolerance of the material [16–18]. Therefore, characterizing and understanding the *R*-curve as well as developing the material which has appropriate *R*-curve behaviour are an effective means of achieving narrow strength distributions, i.e., reliable materials, independent of randomly introduced flaws. However, *R*-curve characterization methods for ceramics are still developing and have not been standardized. A variety of characterization methods exist, and the most widely and favourably used are indentation [19], indentation–crack growth [20, 21], and indentation–strength methods [22]. The advantages of these methods are the relative simplicity and small test specimen volume required. Since the development of silicon nitride with high fracture toughness in excess of 6 MPa $m^{1/2}$, there have been relatively few studies of the *R*-curve as a function of characterization methods.

In this work, the *R*-curve behaviour of two *in situ* reinforced silicon nitrides, A and B, with different microstructures were determined by three widely used characterization methods: indentation, indentation–crack growth, and indentation–strength methods. Silicon nitride A was a commercial, pressureless sintered, *in situ* toughened silicon nitride with relatively fine microstructure, and silicon nitride B was a gas-pressure sintered, *in situ* toughened silicon nitride fabricated from β-Si_3N_4 powder with a relatively coarse microstructure. The results of *R*-curve determinations are presented and the three characterization methods are compared. The results of this work indicate that care should be taken in interpreting and utilizing *R*-curves evaluated from different methods.

2. Experimental procedure

2.1. Materials

The silicon nitride A used in this study was a commercial, pressureless sintered, *in situ* toughened silicon nitride (Referceram SN, Japan Fine Ceramics Centre, Nagoya, Japan). Additives in sintered materials were 3.38 wt % MgO, 4.15 wt % Ce_2O_3, and 0.84 wt % SrO (by atomic absorption spectroscopy). The silicon

* Visiting scientist, on leave from Korea Institute of Science and Technology, Seoul, Korea.

0022–2461

nitride B was fabricated as follows. The raw β-Si_3N_4 powder (Grade SN-P21FC, Denkikagaku, Tokyo, Japan), which was made by nitridation of silicon, and 4 mol% of an equimolar ratio of Al_2O_3 (A16-SG, Alcoa Industrial Chemicals, Bauxite, AR, USA) and Y_2O_3 (99.9% pure, Shin-etsu Chemical, Tokyo, Japan) were ball-milled in ethanol for 24 h, dried, die-pressed at 20 MPa and isostatically pressed at 200 MPa. The green compacts were fired at 2000 °C for 8 h under 1 MPa nitrogen.

Image analysis of the large elongated grains was conducted to evaluate the microstructural features quantitatively. Polished and plasma-etched specimens were examined by scanning electron microscopy (SEM) at magnifications of X1000 and X2000. The length, diameter, and area of each grain were measured by Luzex III (Nireco Corp., Tokyo, Japan). As all grains are basically hexagonal prisms in shape, the diameter of each grain was directly determined from the shortest grain diagonal. The apparent length of each grain was obtained from the longest diagonal.

2.2. *R*-curve measurements

2.2.1. Indentation method

The surface of the specimen was polished well for optical microscopic observation. Prior to indentation, a thin film of gold was deposited on the indentation surface for accurate observation of the crack size and a thin film of moisture-free silicone oil was spread over the site of the indentation for minimizing moisture-assisted subcritical crack growth of as-indented cracks. Vickers indentations were made on the polished surface with indentation loads ranging from 4.9–490 N. The indentation-induced crack lengths, $2c$, were measured with an optical microscope and the crack growth resistance parameter, K_R, was calculated using the following expression proposed by Anstis et al. [19],

$$K_R = \S_v(E/H)^{1/2}(P/c^{3/2}) \quad (1)$$

where $\S_v$ is a material-independent constant for Vickers-produced radial cracks; $\S_v = 0.016$ [19] was used in this study. E, H and P are Young's modulus, Vickers hardness and indentation load, respectively.

2.2.2. Indentation–crack growth method

Specimens for this test were cut and ground to rectangular bars in dimensions of 3 mm × 4 mm × 40 mm with a 140 grit diamond wheel. The tensile surface was polished with 1 μm diamond paste to remove residual stress due to machining and to produce a finish for optical microscopic observation. Prior to indentation, a thin film of gold was deposited on the indentation surface and a thin film of moisture-free silicone oil was spread over the site of indentation. Special care was taken to orient the radial cracks generated from the indentation parallel to the sides of the bar. A Vickers indentation with loads ranging from 4.9–490 N was made at the centre of the prospective tensile surface of each test piece. A total of 12 indented bars for each of A and B were incrementally stressed using four-point bending until cracks reached the critical state. For four-point bending, 10 mm inner and 30 mm outer spans were used. Normally the specimens were stressed to the predetermined peak stress with a cross-head speed of 0.05 mm min^{-1}, and then were unloaded as soon as the peak stress was reached. After each stress increment, the specimen was removed from the fixture and the crack length was measured using optical microscopy.

K_R was calculated as follows. The total stress intensity factor, K_T, for an indentation crack is the sum of the bending stress intensity factor, K_b, and the residual stress intensity factor, K_r [19–21]

$$K_T = K_b + K_r = \sigma Y c^{1/2} + \S_v(E/H)^{1/2}(P/c^{3/2}) \quad (2)$$

where Y and σ are the shape factor of crack geometry and the applied stress, respectively.

A Vickers indentation crack can propagate stably up to ≈2.5 times of its initial length c_o, as long as the following condition is satisfied [19–21]

$$\frac{dK_T}{dc} < \frac{dK_R}{dc} \quad (3)$$

In this stable growth region, a crack stops propagating whenever $K_T = K_R$. Therefore, the R-curve of a material can be obtained by successively increasing the applied stress on a given crack, measuring the crack sizes, and calculating $K_R (= K_T)$ using Equation 2. In this study, the K_R value based on the first crack opening at each indentation load was not contained in plotting the R-curve, because it may be affected by residual stress formed in the specimen. Also, the values of Y and $\S_v$ were assumed as constants, 1.174 [22] and 0.016 [19], respectively.

2.2.3. Indentation–strength method

Specimens for this test were prepared as for the indentation–crack growth method. Three Vickers indentations with loads ranging from 2.94–490 N were made 3 mm apart in the centre of prospective tensile surface of each test piece. A total of ≈30 indented bars for each of A and B were directly fractured using four-point bending. The strength data of specimens that fractured from the indented sites were used for the subsequent R-curve analysis [22] described as follows. In this analysis, an analytical function of crack extension, Δc, to a fractional power is used to represent the fracture resistance, K_R, as follows

$$K_R = k(\Delta c)^m \quad (4)$$

where k and m are constants. Then, the relation between the strength, S, and the indentation load, P, is given as follows

$$\log S = \log \alpha - \beta \log P \quad (5)$$

where the exponent β is defined by

$$\beta = (1 - 2m)/(2m + 3) \quad (6)$$

and the coefficient α is defined by

$$\alpha = kY^{-1}(\beta\gamma)^{\beta}(1 + \beta)^{(-1+\beta)} \quad (7)$$

In Equation 7, the constant γ is defined by

$$\gamma = P/(c_1)^{2/(1+\beta)} \quad (8)$$

where c_1 is the initial crack length due to indentation. The crack length at the onset of instability, c_T, is given by

$$c_T = c_1[4/(1 - 2m)]^{2/(3+2m)} \quad (9)$$

An R-curve is generated by plotting $\log S$ versus $\log P$. From this plot, the constants α and β can be determined from the intercept and the slope, respectively. The constants m and k can then be calculated utilizing Equations 6 and 7, respectively. In calculating constant k, it is necessary to determine the constant γ. For this calculation, Equation 8 is utilized. By taking the logarithm of Equation 7 and plotting $\log c_1$ versus $\log P$, the constant γ can be determined from the intercept. With the use of Equation 4, a plot of K_R versus Δc can be made, where $\Delta c = c_T$, as given by Equation 9. Details of the analytical procedure to obtain the R-curve were described by Krause [22].

3. Results and discussion

3.1. Microstructure evaluation

Silicon nitrides A and B have single-edge precracked-beam (SEPB) [23] toughnesses of 7.0 and 8.0 MPa $m^{1/2}$, respectively, and Young's modulus of 290 GPa for both materials. Both materials were nearly 100% dense.

Scanning electron micrographs of polished and plasma-etched surfaces are shown in Fig. 1. As shown, both specimens had an *in situ* composite microstructure consisting of small matrix grains and large elongated grains. However, silicon nitride B had a coarser microstructure.

Image analysis of the large elongated grains was conducted to evaluate the microstructure quantitatively. Image analysis of the small matrix grains was not considered, because the contribution of small matrix grains to the fracture resistance was minor compared to that of the large elongated grains. It was difficult to evaluate occasional very large grains in silicon nitride B statistically, and they were thus excluded in present treatment. The grain-diameter distribution and aspect-ratio distribution for each material were obtained. Grain diameter was evaluated as the thickness observed in a two-dimensional cross-section. The frequency distribution was expressed in terms of the percentage of the total area occupied by grains of the same diameter size. An area per cent expression in a two-dimensional observation approximately corresponds to volume per cent in a three-dimensional observation [24]. Fig. 2 shows the grain-diameter distribution for silicon nitrides A and B. Silicon nitride A had an elongated grain-diameter distribution from 0.4–2.2 μm. On the other hand, silicon nitride B had an elongated grain-diameter distribution from 0.8–7.2 μm. The average aspect ratio (grain length/grain diameter) of large elongated grains was estimated for both materials. The aspect ratio measured in a two-dimensional cross-section is not equal to the true aspect ratio in three dimensions. In such case, the mean value of the 10% highest observed ratio was shown to be the mean of the real aspect ratio [3, 25]. Table I shows the average diameter and the average apparent length of large elongated grains and the calculated average aspect ratio for both materials. The results show that silicon nitrides A and B have a similar aspect ratio, but silicon nitride B has a diameter approximately twice that of silicon nitride A.

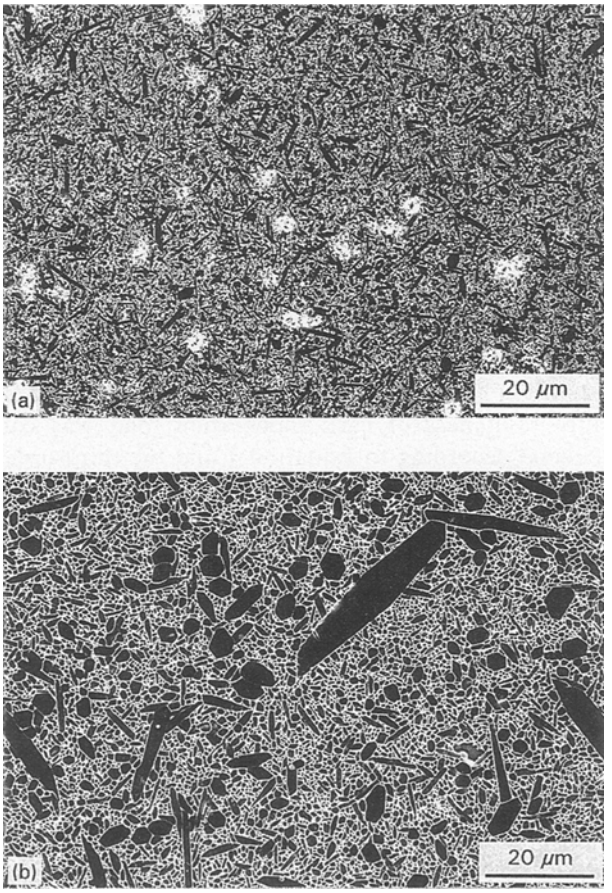

Figure 1 Typical microstructures of polished and etched silicon nitride surfaces: (a) A and (b) B.

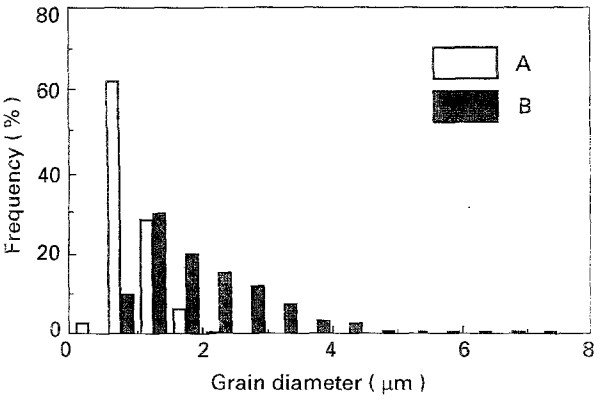

Figure 2 Grain-diameter distribution of large elongated grains in silicon nitrides A and B.

3.2. R-curve behaviour

The results of fracture resistance measurements as a function of crack length for the three methods are

TABLE I Average diameter, average apparent length and average aspect ratio of large elongated grains in silicon nitrides A and B

Material	Average diameter (μm)	Average apparent length (μm)	Average aspect ratio[a]
A	0.95	2.89	5.6
B	2.01	5.49	5.9

[a] The mean value of the 10% highest observed aspect ratios.

shown in Fig. 3. For the indentation method, the fracture toughness of each indentation load was calculated according to Equation 1 and the third-order polynomials were fitted to the data for silicon nitrides A and B and the results are shown as a function of crack length in Fig. 3a. For the measured crack range, silicon nitride B has a higher fracture toughness than silicon nitride A. The toughness becomes higher as the crack length increases, and the third-order polynomials extrapolate to intrinic toughness $K_0 \approx 3.06$ and 3.69 MPa $m^{1/2}$ at $c = 0$ for silicon nitrides A and B, respectively. The saturated crack growth resistances were 5.2 and 5.8 MPa $m^{1/2}$ for silicon nitride A and B, respectively.

For the indentation–crack growth method, the third-order polynomials were fitted to the data for silicon nitrides A and B, respectively, and are shown in Fig. 3b. The polynomial R-curves extrapolate to $K_0 \approx 4.19$ and 5.07 MPa $m^{1/2}$ at $c = 0$ for silicon nitrides A and B, respectively. These K_0 values may be too high because a chemical-vapour deposited single-crystal silicon nitride has a fracture toughness of 1.9–2.8 MPa $m^{1/2}$ measured by the indentation method [26]. As shown in Fig. 3b, silicon nitride B has higher values of K_R than silicon nitride A in the measured crack-size range between 30 and 500 μm. This trend is consistent with the results of indentation fracture toughness measured at each indentation load (Fig. 3a) although the absolute values are different. The saturated crack-growth resistances were 7.2 and 8.0 MPa $m^{1/2}$ for silicon nitride A and B, respectively.

For the indentation–strength method, a plot of the logarithm of fracture strength of indented bars versus the logarithm of indentation load was used for determining α and β in Equation 5. Linear regression was used to obtain the best fit lines for the data from silicon nitrides A and B and slopes of silicon nitrides A and B were 0.285 70 and 0.229 61, respectively. Griffith materials which show no R-curve behaviour have a slope of 1/3 and R-curve materials have lower slopes [22]. Because the slopes of both materials are less than 1/3, the rising R-curve behaviour is evident for both materials. Every specimen was checked to ensure that fracture was initiated from the indent. Estimated values of constants k and m were 13.9 and 0.0556 for silicon nitride A and 24.3 and 0.1265 for silicon nitride B, respectively. As shown in Fig.3c, silicon nitride B showed more pronounced R-curve behaviour than silicon nitride A. However, silicon nitride A showed higher K_R if the crack extension was less than 400 μm. This result is different from those obtained by indentation and indentation–crack growth methods. The saturated crack-growth resistances were 9.2 and 10.0 MPa $m^{1/2}$ for silicon nitrides A and B, respectively.

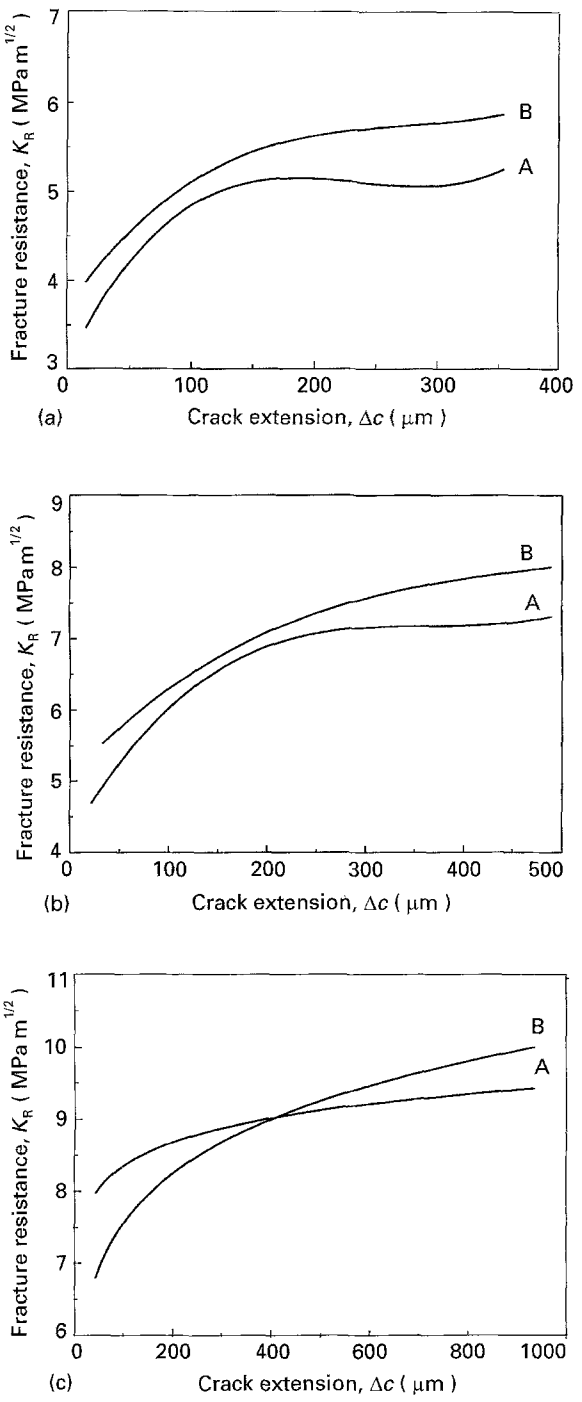

Figure 3 Rising crack-growth resistance curves (R-curve) as a funtion of crack size for silicon nitrides A and B: (a) indentation method, (b) indentation–crack growth method, and (c) indentation–strength method.

All of the three methods showed rising crack-growth resistance behaviour, i.e., R-curves for both materials. However, the K_R values and the rising behaviour were different among three methods. The indentation method showed the lowest K_R of the three. This may be caused by the following two reasons. Because the crack extension of the indentation method is relatively shorter than those of the others two methods, the measured K_R should be lower than

those of others which have longer crack extension. Also, the indentation crack is introduced by a specific stress field and it has a relatively fast crack extension velocity. Rapid crack extension may have limited bridge formation, i.e. limited crack shielding. The indentation–strength method showed the highest of K_R obtained from the three test methods. This may be caused by the longer crack extension. However, the magnitude of K_R is very sensitive to the constants, k and m, and it is difficult to estimate the constants accurately because they are strongly dependent on the strength data. The K_R value obtained from the indentation–crack growth method is in between those of the indentation method and the indentation–strength method. Also, the saturated K_R values obtained for silicon nitrides A and B at large crack extension were consistent with the SEPB toughness measured for them. From the above results, it is seen that not only do the measured K_R values differ depending on the method, but a relative comparison also cannot be made because the indentation–strength method shows different behaviour from the other two methods if the crack size is less than 400 μm. The rising behaviour of R-curve as well as the K_R value are, also, very important for characterizing the materials because the slope of the R-curve behaviour around a crack size about that of a natural flaw, is related with the reliability of the materials [16–18]. In fact, the R-curve behaviour within 200 μm of the crack extension is very important, because the critical flaw size of the silicon nitride materials is usually less than 200 μm [27]. However, the results obtained from the three methods do not coincide if the crack size is less than 200 μm, and not provide any conclusion.

The damage tolerance could be estimated from the strength data of indented bars. In Fig. 4, bending strength for silicon nitride A reached its natural strength at 2.94 N indentation. However, the bending strength for silicon nitride B reached its natural strength at 4.9 N indentation. This result suggests that silicon nitride B, which has coarser microstructure, is a more damage-tolerant material than silicon nitride A. It is also supported by the crossover of strength, which takes place between 49 and 98 N. Initially silicon nitride A has about 23% higher strength than silicon nitride B. However, after 98 N indentation, silicon nitride A loses about 66% of its initial strength, while silicon nitride B loses about 52% of its initial strength and becomes a stronger material than silicon nitride A. Large elongated grains in silicon nitride with coarser microstructure are believed to act as fracture origins [5]. Because silicon nitride B has a coarser microstructure, its critical flaw size may be larger than that of silicon nitride A. Hence, it is reasonable that silicon nitride B is more damage tolerant than silicon nitride A. The above results also suggest that silicon nitride B may have higher K_R than silicon nitride A.

Strictly speaking, there is no unique fracture toughness value for rising R-curve materials. Therefore, the evaluation of the R-curve is essential for R-curve materials. However, R-curve measuring methods are still not standardized and existing methods, sometimes,

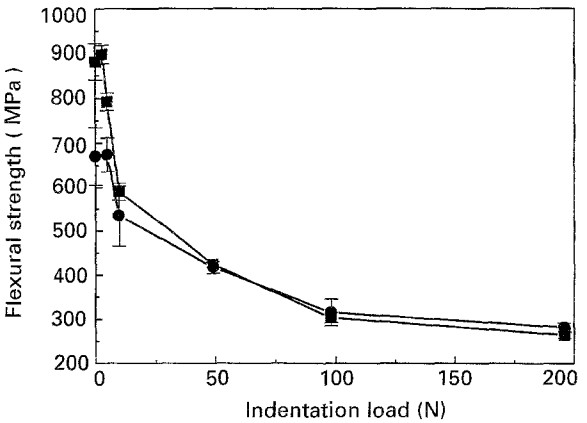

Figure 4 Plots of strength, S, versus indentation load, P, for silicon nitrides (■) A and (●) B.

lead to different results. The R-curve behaviour measured from indentation–crack growth and indentation–strength methods, for example, result in a discrepancy in rising behaviour and K_R values for both silicon nitrides A and B. It is thus suggested that at least two testing methods, such as indentation–crack growth and indentation–strength methods, are needed when evaluating the fracture resistance of *in situ* toughened silicon nitrides. In addition, care should be taken in interpreting and utilizing R-curves evaluated by different methods. Standardization of R-curve evaluation methods as well as the toughness measuring method is also needed.

4. Conclusion

R-curves for two *in situ* reinforced silicon nitrides A and B of different microstructures were determined by three different characterization methods. The values of saturated crack-growth resistance were found to be 5.2, 7.2 and 9.2 MPa $m^{1/2}$ for silicon nitride A and 5.8, 8.0 and 10.0 MPa $m^{1/2}$ for silicon nitride B, respectively, by indentation, indentation–crack growth, and indentation–strength methods. The rising behaviour of the R-curves was also found to depend on the characterization method. These results suggest that care should be taken in interpreting and utilizing R-curves evaluated from different characterization methods and an R-curve characterization method with appropriate qualifiers is needed for rising R-curve materials.

Acknowledgement

This work was supported by the Japan–Korea Cooperation Foundation for Industry and Technology (JKF). Also, the residence of Dr. Kim in NIRIM.

References

1. P. F. BECHER, C. HSUEH, P. ANGELINI and T. N. TIEGS, *J. Am. Ceram. Soc.* **71** (1988) 1050.
2. K. T. FABER and A. G. EVANS, *Acta Metall.* **31** (1983) 565.
3. M. MITOMO, M. TSUTSUMI, H. TANAKA, S. UENOSONO and F. SAITO, *J. Am. Ceram. Soc.* **73** (1990) 2441.

4. N. HIROSAKI, M. ANDO, Y. AKIMUNE and M. MITOMO, *J. Ceram. Soc. Jpn* **100** (1992) 826.
5. N. HIROSAKI, Y. AKIMUNE and M. MITOMO, *J. Am. Ceram. Soc.* **76** (1993) 1892.
6. *Idem, ibid.* **77** (1994) 1093.
7. F. F. LANGE, *ibid.* **56** (1973) 518.
8. E. TANI, S. UMEBAYASHI, K. KISHI, K. KOBAYASHI and M. NISHIJIMA, *Am. Ceram. Soc. Bull.* **65** (1986) 1311.
9. M. MITOMO and K. MIZUNO, *Yogyo Kyokaishi* **94** (1986) 106.
10. N. RAMACHANDRAN and D.K. SHETTY, *J. Am. Ceram. Soc.* **74** (1991) 2634.
11. H. E. SALIBA, L. CHUCK and N. L. HECHT, *Ceram. Eng. Sci. Proc.* **12** (1991) 1418.
12. C. W. LI, D. J. LEE and S. C. LUI, *J. Am. Ceram. Soc.* **75** (1992) 1777.
13. D. B. MARSHALL, *ibid.* **69** (1986) 173.
14. A. REICHL and R. W. STEINBRECH, *J. Am. Ceram. Soc.* **71** (1988) C299.
15. R. F. KRAUSE, E. R. FULLER and J. F. RHODES, *ibid.* **73** (1990) 559.
16. R. F. COOK and D. R. CLARKE, *Acta Metall.* **36** (1988) 555.
17. D. K. SHETTY and J. S. WANG, *J. Am. Ceram. Soc.* **72** (1989) 1158.
18. S. J. BENNISON and B. R. LAWN, *J. Mater. Sci.* **24** (1989) 3169.
19. G. R. ANSTIS, P. CHANTIKUL, B. R. LAWN and D. B. MARSHALL, *J. Am. Ceram. Soc.* **64** (1981) 533.
20. D. B. MARSHALL and B. R. LAWN, *J. Mater. Sci.* **14** (1979) 2001.
21. P. CHANTIKUL, G. R. ANSTIS, B. R. LAWN and D. B. MARSHALL, *J. Am. Ceram. Soc.* **64** (1981) 539.
22. R. F. KRAUSE, *ibid.* **71** (1988) 338.
23. T. NOSE and T. FUJII, *ibid.* **71** (1988) 328.
24. N. HIROSAKI, Y. AKIMUNE and M. MITOMO, *J. Ceram. Soc. Jpn* **101** (1993) 1239.
25. G. WÖTTING, B. KANKA and G. ZIEGLER, in "Non-oxide technical and engineering ceramics," edited by S. Hampshire (Elsevier, London, 1986) p. 83.
26. H. SUEMATSU, J. J. PETROVIC and T. E. MITCHELL, in "Silicon nitride ceramics: scientific and technological advances," edited by I.-Wei Chen, P. F. Becher, M. Mitomo, G. Petzow and T. S. Yen, Materials Research Society Symposium Proceedings 287, (MRS, Pittsburgh, PA, 1993) p. 449.
27. Y. W. KIM, M. MITOMO and N. HIROSAKI, *J. Mater. Res.* (1994) in print.

Received 5 September 1994
and accepted 21 February 1995